









Comparison of the Imaging Features of Lobular Carcinoma In Situ and Invasive Lobular Carcinoma of the Breast

유방의 소엽상피내암과 침윤성 소엽암의
영상의학적 소견 비교

Ga Young Yoon, MD¹ , Joo Hee Cha, MD^{2*} , Hak Hee Kim, MD² ,
Min Seo Bang, MD³ , Hee Jin Lee, MD⁴ , Gyungyub Gong, MD⁴ 

¹Department of Radiology, Gangneung Asan Hospital, University of Ulsan College of Medicine, Gangneung, Korea

Departments of ²Radiology and Research Institute of Radiology and ⁴Pathology, Asan Medical Center, University of Ulsan College of Medicine, Seoul, Korea

³Department of Radiology, Ulsan University Hospital, University of Ulsan College of Medicine, Ulsan, Korea

Purpose To investigate the usefulness of imaging features for differentiating between small lobular carcinoma in situ (LCIS) and invasive lobular carcinoma (ILC).

Materials and Methods It included 52 female with LCISs (median 45 years, range 32–67 years) and 180 female with ILCs (median 49 years, range 36–75 years), with the longest diameter of ≤ 2 cm, who were evaluated between January 2012 and December 2016. All the female underwent mammography and ultrasonography. Twenty female with LCIS and 150 female with ILC underwent MRI. The clinical and imaging features were compared, and multivariate analysis was performed to identify the independent predictors of LCIS. Female with LCIS were also subgrouped by lesion size and compared with the female with ILC.

Results Multivariate analysis showed that younger age (odds ratio [OR] = 1.100), smaller lesion size (OR = 1.103), oval or round shape (OR = 4.098), parallel orientation (OR = 5.464), and isoechotexture (OR = 3.360) were significant independent factors predictive of LCIS. The area under the receiver operating characteristic curve for distinguishing LCIS from ILC was 0.904 (95% confidence interval, 0.857–0.951). Subgroup analysis showed that benign features were more prevalent in female with smaller LCISs (≤ 1 cm) than in those with ILC.

Conclusion Small LCISs tend to demonstrate more benign features than small ILCs. Several imaging features are independently predictive of LCIS.

Index terms Breast Neoplasms; Carcinoma, Lobular; Mammography; Ultrasonography; Magnetic Resonance Imaging

Received August 11, 2020
Revised October 23, 2020
Accepted January 14, 2021

*Corresponding author

Joo Hee Cha, MD
Department of Radiology and
Research Institute of Radiology,
Asan Medical Center,
University of Ulsan
College of Medicine,
88 Olympic-ro 43-gil, Songpa-gu,
Seoul 05505, Korea.


Tel 82-2-3010-5995

Fax 82-2-476-0090

E-mail jhcha@amc.seoul.kr

This is an Open Access article distributed under the terms of the Creative Commons Attribution Non-Commercial License (<https://creativecommons.org/licenses/by-nc/4.0>) which permits unrestricted non-commercial use, distribution, and reproduction in any medium, provided the original work is properly cited.

ORCID iDs

Ga Young Yoon 


[https://](https://orcid.org/0000-0003-0933-1570)

orcid.org/0000-0003-0933-1570

Joo Hee Cha 


[https://](https://orcid.org/0000-0002-1446-8195)

orcid.org/0000-0002-1446-8195

Hak Hee Kim 


[https://](https://orcid.org/0000-0002-2956-9212)

orcid.org/0000-0002-2956-9212

Min Seo Bang 


[https://](https://orcid.org/0000-0001-8933-1444)

orcid.org/0000-0001-8933-1444

Hee Jin Lee 

[https://](https://orcid.org/0000-0002-4963-6603)

orcid.org/0000-0002-4963-6603

Gyungyub Gong 

[https://](https://orcid.org/0000-0001-5743-0712)

orcid.org/0000-0001-5743-0712

INTRODUCTION

Lobular carcinoma in situ (LCIS) is defined as a monomorphic population of small and loosely cohesive cells that expand the terminal ductal lobular unit, with or without pagetoid involvement of terminal ducts (1). The American Joint Committee on Cancer 8th edition (2) does not classify LCIS as a Tis because it is considered a risk factor for malignancy, not a malignancy itself. By contrast, invasive lobular carcinoma (ILC) is defined as an invasive carcinoma, often associated with LCIS, and the second most common histopathologic subtype of breast cancer (3). Although LCIS and ILC show significant similarities on the genetic and molecular levels (4-6), their treatments are quite different. According to National Comprehensive Cancer Network guidelines (7), female with early-stage ILC should undergo primary surgery with or without radiation therapy. Although the importance of LCIS as a risk indicator or a direct precursor of ILC remains unclear (8-12), recent guidelines suggest that patients with “classic” LCIS do not require surgical treatment, and that female with LCIS diagnosed by core needle biopsy receive counseling regarding the risk reduction of developing invasive cancer (7).

LCIS has been regarded as clinically undetectable, with its diagnosis often considered an incidental finding (13, 14). Although calcifications on mammography (14, 15), and foci or non-mass enhancement (NME) on MRI (16), have been reported to correlate with lobular neoplasia on core needle biopsy, the imaging features of LCIS are not yet well-established. Imaging features that can differentiate LCIS from ILC, especially small-sized LCIS and ILC, could help guide treatment and predict prognosis in female with these lesions. This study therefore investigated whether imaging features are useful for differentiating between small-sized LCIS and ILC.

MATERIALS AND METHODS

PATIENT SELECTION

This retrospective study from a single tertiary center was approved by the Institutional Review Board, which waived the requirement for informed patient consent (IRB No. 2019-0290). Female were included if they had been diagnosed with LCIS or ILC by surgery between January 2012 and December 2016, and if the longest diameter of the surgically removed lesion was ≤ 2 cm. Female with pure LCIS, as well as those with concurrent flat epithelial atypia (FEA) and/or a columnar cell lesion, were included (17, 18). To exclude the cases which were incidentally detected LCIS, cases with separate major lesions in the final pathology were excluded and only lesions that could explain LCIS as the pathology for imaging or pathology were included. Male patients, female of younger (< 19 years) and older (> 75 years) age, patients with pleomorphic LCIS, and those with tumors > 2 cm in diameter were excluded.

IMAGING TECHNIQUE

A full-field distal mammography system (Senographe Essential; GE Healthcare, Milwaukee, WI, USA) was used to obtain images in two standard planes. Breast ultrasound (US) was performed by radiologists using high-resolution US equipment with a 14–16 MHz linear ar-

ray transducer (iU 22; Philips Healthcare, Bothell, WA, USA).

Breast MRI was performed using a 1.5T (Avanto; Siemens Medical Solutions, Erlangen, Germany) or a 3.0T (Skyra; Siemens Medical Solutions or Ingenia; Philips, Best, the Netherlands) MR scanner, and a dedicated 18-channel phased-array breast coil with the patient in a prone position. The imaging protocol included a T2-weighted sequence (1.5T: repetition time [TR]/echo time [TE], 1300/131; field of view [FOV], 340 × 340 mm; matrix size, 384 × 384; and slice thickness, 1.5 mm; 3.0T: TR/TE, 1100/131; FOV, 341 × 210 mm; matrix size, 256 × 416; and section thickness, 1.5 mm) and a dynamic contrast material-enhanced fat-suppressed T1-weighted sequence (1.5T: TR/TE, 5.0/2.4; FOV, 340 × 340 mm; matrix size, 384 × 384; section thickness, 0.9 mm; 3.0T: TR/TE, 5.6/2.5; FOV, 360 × 360 mm; matrix size, 384 × 384; section thickness, 0.9 mm), consisting of one unenhanced and five contrast-enhanced acquisitions, with a temporal resolution of 61 seconds. For all examinations, 0.2 mL/kg gadoterate meglumine (UNIRAY®; Dongkook Pharmaceutical Co., Ltd, Seoul, Korea) was power-injected (Spectris; Medrad, Pittsburgh, PA) at a flow rate of 1 mL/s, followed by a 20 mL saline flush.

IMAGE ANALYSIS

Two breast radiologists (with 20 and 5 years of clinical experience in breast imaging, respectively) retrospectively reviewed. Each radiologist independently reviewed images without knowledge of the clinical and histopathological data, based on the American College of Radiology (ACR) breast imaging reporting and data system (BI-RADS) 5th edition lexicon (19). Discrepancies were resolved by a consensus of the two radiologists reviewing the case together. Female were also subgrouped by lesion size, ≤ 1 cm and > 1 cm.

On mammography, lesions were classified as not seen, mass or calcification only, or mass with calcification; there was no architectural distortion or asymmetry. Mass lesions were evaluated by shape and margin, and areas of calcification were analyzed by morphology and distribution. Mammographic breast density was also determined, based on the four categories of breast composition described by the ACR BI-RADS.

On US, the recorded data included lesion type (not seen, mass, non-mass, mixed), multifocality or multicentricity, mass shape, orientation, margins, echo pattern, posterior features, and vascularity. A nonmass at US is defined as a discrete area of altered echotexture compared with the surrounding breast tissue (20). Also, a mixed lesion means that the lesion shows both mass and nonmass.

On MRI, the data recorded included the extent of background parenchymal enhancement (BPE; minimal, mild, moderate, or marked), and lesion multifocality, multicentricity, and morphologic features. Lesion type was classified as not seen, mass, NME, or mass with NME. Masses were classified according to shape, margins, and internal enhancement. The presence of high intratumoral signal intensity (SI) and peritumoral edema was also evaluated on fat-suppressed T2-weighted images (T2WI). High intratumoral SI on T2WI was defined as tumor SI higher than or almost the same as SI of water or vessels, or higher than that of the surrounding normal parenchymal tissue (21). Peritumoral edema was defined as high SI around the tumor on T2WI (22). NMEs were analyzed by determining their distribution and internal enhancement. The kinetic features of each tumor were evaluated using a commercially available computer-aided diagnosis (CAD) system (CADstream, version 6.0.1; Confirma

Inc., Kirkland, WA, USA).

CLINICOPATHOLOGIC ANALYSIS

All histopathological information was obtained from the pathology reports. All resected specimens were histopathologically verified, and the cancer type and tumor characteristics, such as pathologic tumor size on gross specimen, hormone receptor status, and presence of concurrent FEA or columnar cell lesion, were evaluated. Demographic and clinical factors were also evaluated, including age at diagnosis, menopausal status, marital status, childbirth, use of contraception, hormone replacement therapy, history of breast cancer, and family history of breast cancer.

STATISTICAL ANALYSIS

Continuous variables are reported as median with interquartile range, whereas categorical variables are reported as frequencies and percentages. The clinical and imaging characteristics of the LCIS and ILC groups were compared using Mann-Whitney U-tests for continuous variables, and chi-square or Fisher's exact test for categorical variables. Univariate and multivariate analyses were performed to identify significant independent factors associated with LCIS. Imaging variables on MRI were excluded from the univariate and multivariate analyses due to a lack of sufficient data. All variables with a p value < 0.001 on univariate analyses were included in the multivariate analysis, with backward elimination used to arrive at the final model. The model was internally validated using a bootstrap resampling procedure. Receiver operating characteristic (ROC) curve analysis was performed to evaluate the diagnostic performance of the factors for distinguishing between the LCIS and ILC groups, and areas under the ROC curves were calculated. A p value < 0.05 was considered statistically significant. All statistical analyses were performed using R software, version 3.5.1 (R Foundation for Statistical Computing, Vienna, Austria).

RESULTS

Fifty-two female with LCIS (34 with pure LCIS lesions and 18 with LCIS lesions and concurrent FEA and/or columnar cell lesion) and 180 female with ILC were included in this analysis. Of 52 female with LCIS, the initial methods for pathologic confirmation were US-guided core needle biopsy ($n = 29$), US-guided vacuum assisted biopsy ($n = 6$), stereotactic biopsy ($n = 12$), and excisional biopsy ($n = 5$). Of 180 female with ILC, the initial methods for pathologic confirmation were US-guided core needle biopsy ($n = 177$), US-guided vacuum assisted biopsy ($n = 1$), stereotactic biopsy ($n = 1$), and excisional biopsy ($n = 1$). The clinical characteristics of the LCIS and ILC groups are summarized in Table 1. Median age at diagnosis was significantly lower in female with LCIS than with ILC (45 years [range, 32–67 years] vs. 49 years [range, 36–75 years], $p < 0.001$). Premenopausal status was significantly more frequent in patients with LCIS than with ILC ($p = 0.005$). None of the other clinical characteristics differed significantly in the LCIS and ILC groups.

All female underwent mammography and US. Twenty female with LCIS and 150 with ILC underwent MRI. Table 2 shows the mammographic features of the LCIS and ILC groups.

Table 1. Clinical Characteristics of Female with LCISs and ILCs

	Total			Lesion Size ≤ 1 cm			Lesion Size > 1 cm		
	LCIS (n = 52)	ILC (n = 180)	p	LCIS (n = 39)	ILC (n = 42)	p	LCIS (n = 13)	ILC (n = 138)	p
Age, year	45 [32–67]	49 [36–75]	<0.001	45.0 [43.0–49.0]	46.0 [44.0–53.0]	0.172	46.0 [42.0–48.0]	49.0 [46.0–55.0]	0.025
Pathologic lesion size, mm	8.0 [4.0–10.5]	14.0 [11.0–17.0]	<0.001	6.0 [3.5–8.0]	7.0 [6.0–9.0]	0.105	15.0 [12.0–18.0]	15.0 [13.0–18.0]	0.667
Premenopausal	43 (82.7)	109 (60.6)	0.005	33 (84.6)	27 (64.3)	0.045	10 (76.9)	82 (59.4)	0.251
Married	44 (84.6)	166 (92.2)	0.167	33 (84.6)	37 (88.1)	0.751	11 (84.6)	129 (93.5)	0.241
Childbirth	43 (82.7)	157 (87.2)	0.544	32 (82.1)	35 (83.3)	>0.999	11 (84.6)	122 (88.4)	0.655
Use of contraceptive	11 (21.2)	23 (12.8)	0.200	6 (15.4)	8 (19.1)	0.772	5 (38.5)	15 (10.9)	0.016
Hormone replacement	2 (3.9)	16 (8.9)	0.366	1 (2.6)	2 (4.8)	>0.999	1 (7.7)	14 (10.1)	>0.999
History of breast cancer	0 (0.0)	3 (1.7)	0.810	0 (0.0)	0 (0.0)		0 (0.0)	3 (2.2)	>0.999
Family history of breast cancer	12 (23.1)	21 (11.7)	0.064	11 (28.2)	7 (16.7)	0.286	1 (7.7)	14 (10.1)	>0.999

Results are reported as median [range] or number (percentage) of patients.

ILC = invasive lobular carcinoma, LCIS = lobular carcinoma in situ

Overall, 20 of 52 (38.5%) female in the LCIS group had lesions not seen on mammography, whereas 110 of 180 (61.1%) female in the ILC group presented with mass-only lesions on mammography ($p < 0.001$). If masses were present, those in the LCIS group were significantly more likely than those in the ILC group to be oval or round in shape, and have circumscribed margins ($p < 0.001$) (Fig. 1). Most masses in the ILC group were irregular in shape and had spiculated margins (Fig. 2). Calcifications on mammography were significantly more frequent in the LCIS than in the ILC group (44.2% [23/52] vs. 17.2% [31/180], $p < 0.001$). If calcifications were present, lesions in the LCIS group were more likely than those in the ILC group to show an amorphous morphology ($p < 0.001$) (Fig. 3). Grouped distribution of calcifications was more common in both groups. Mammographic breast density did not differ significantly in the two groups.

On US, most tumors in both groups appeared as masses without vascularity (Table 3). Except for mass type, LCISs tended to be not seen on US ($p < 0.001$). Lesions present in the LCIS group were significantly more likely to be oval or round in shape ($p < 0.001$); to have a parallel orientation ($p = 0.002$), circumscribed or microlobulated margins ($p < 0.001$), and a hypo- or isoechotexture ($p < 0.001$); and to be lacking posterior features ($p < 0.001$) than lesions in the ILC group (Fig. 1).

Breast MRI showed significant differences in the LCIS and ILC groups (Table 4), including lesion type ($p < 0.001$), mass shape ($p = 0.023$), mass margin ($p = 0.001$), and NME internal enhancement ($p = 0.031$) and kinetics ($p < 0.001$). LCIS lesions tended to be oval or round in shape, be circumscribed masses or NME with homogeneous enhancement, and have persistent kinetics (Fig. 1), whereas ILCs tended to be irregular in shape, be irregular or spiculated masses or NME with heterogeneous enhancement, and have washout kinetics (Fig. 2). Other imaging features, including BPE, multifocality or multicentricity, mass internal enhance-

Table 2. Mammographic Features of Female with LCISs and ILCs

	Total			Lesion Size ≤ 1 cm			Lesion Size > 1 cm		
	LCIS (n = 52)	ILC (n = 180)	p	LCIS (n = 39)	ILC (n = 42)	p	LCIS (n = 13)	ILC (n = 138)	p
Breast density			0.047			0.361			0.696
Fatty	2/52 (3.9)	28/180 (15.6)		1/39 (2.6)	4/42 (9.5)		1/13 (7.7)	24/138 (17.4)	
Dense	50/52 (96.2)	152/180 (84.4)		38/39 (97.4)	38/42 (90.5)		12/13 (92.3)	114/138 (82.6)	
Lesion type			< 0.001			0.015			0.004
Not seen	20/52 (38.5)	39/180 (21.7)		14/39 (35.9)	18/42 (42.9)		6/13 (46.2)	21/138 (15.2)	
Mass only	9/52 (17.3)	110/180 (61.1)		5/39 (12.8)	14/42 (33.3)		4/13 (30.8)	96/138 (69.6)	
Calcification only	19/52 (36.5)	10/180 (5.6)		17/39 (43.6)	6/42 (14.3)		2/13 (15.4)	4/138 (2.9)	
Mass with calcification	4/52 (7.7)	21/180 (11.7)		3/39 (7.7)	4/42 (9.5)		1/13 (7.7)	17/138 (12.3)	
Mass shape			< 0.001			0.078			0.068
Oval or round	7/13 (53.9)	13/131 (9.9)		5/8 (62.5)	4/18 (22.2)		2/5 (40.0)	9/113 (8.0)	
Irregular	6/13 (46.2)	118/131 (90.1)		3/8 (37.5)	14/18 (77.8)		3/5 (60.0)	104/113 (92.0)	
Mass margin			< 0.001			< 0.001			0.482
Circumscribed	4/13 (30.8)	0/131 (0.0)		4/8 (50.0)	0/18 (0.0)		0/5 (0.0)	0/113 (0.0)	
Obscured	0/13 (0.0)	6/131 (4.6)		0/8 (0.0)	0/18 (0.0)		0/5 (0.0)	6/113 (5.3)	
Microlobulated	3/13 (23.1)	7/131 (5.3)		2/8 (25.0)	1/18 (5.6)		1/5 (20.0)	6/113 (5.3)	
Indistinct	2/13 (15.4)	22/131 (16.8)		1/8 (12.5)	1/18 (5.6)		1/5 (20.0)	21/113 (18.6)	
Spiculated	4/13 (30.8)	96/131 (73.3)		1/8 (12.5)	16/18 (88.9)		3/5 (60.0)	80/113 (70.8)	
Calcification			< 0.001			0.013			0.436
Absent	29/52 (55.8)	149/180 (82.8)		19/39 (48.7)	32/42 (76.2)		10/13 (76.9)	117/138 (84.8)	
Present	23/52 (44.2)	31/180 (17.2)		20/39 (51.3)	10/42 (23.8)		3/13 (23.1)	21/138 (15.2)	
Calcification morphology			< 0.001			0.001			0.143
Amorphous	10/23 (43.5)	2/31 (6.5)		9/20 (45.0)	0/10 (0.0)		1/3 (33.3)	2/21 (9.5)	
Coarse heterogeneous	2/23 (8.7)	2/31 (6.5)		1/20 (5.0)	1/10 (10.0)		1/3 (33.3)	1/21 (4.8)	
Fine pleomorphic	6/23 (26.1)	26/31 (83.9)		5/20 (25.0)	9/10 (90.0)		1/3 (33.3)	17/21 (81.0)	
Fine linear or fine-linear branching	0/23 (0.0)	1/31 (3.2)		0/20 (0.0)	0/10 (0.0)		0/3 (0.0)	1/21 (4.8)	
Others	5/23 (21.7)	0/31 (0.0)		5/20 (25.0)	0/10 (0.0)		0/3 (0.0)	0/21 (0.0)	
Calcification distribution			0.528			0.267			0.723
Diffuse	1/23 (4.4)	0/31 (0.0)		1/20 (5.0)	0/10 (0.0)		0/3 (0.0)	0/21 (0.0)	
Regional	5/23 (21.7)	5/31 (16.1)		5/20 (25.0)	1/10 (10.0)		0/3 (0.0)	4/21 (19.1)	
Grouped	14/23 (60.9)	19/31 (61.3)		12/20 (60.0)	5/10 (50.0)		2/3 (66.7)	14/21 (66.7)	
Segmental	3/23 (13.1)	7/31 (22.6)		2/20 (10.0)	4/10 (40.0)		1/3 (33.3)	3/21 (14.3)	

Results are reported as the number (percentage) of patients.

ILC = invasive lobular carcinoma, LCIS = lobular carcinoma in situ

ment, NME distribution, intratumoral high SI on T2WI, and peritumoral edema on T2WI, did not differ significantly in the LCIS and ILC groups.

Univariate analysis showed that younger age, smaller lesion size, premenopausal status, unseen lesion or calcification alone on mammography, oval or round shape, circumscribed lesions, isoechoic mass and parallel orientation on US were significantly associated with LCIS ($p < 0.1$) (Supplementary Table 1 in the online-only Data Supplement). Multivariate analysis showed that younger age (odds ratio [OR] = 1.100, $p = 0.013$), smaller lesion size (OR = 1.103,

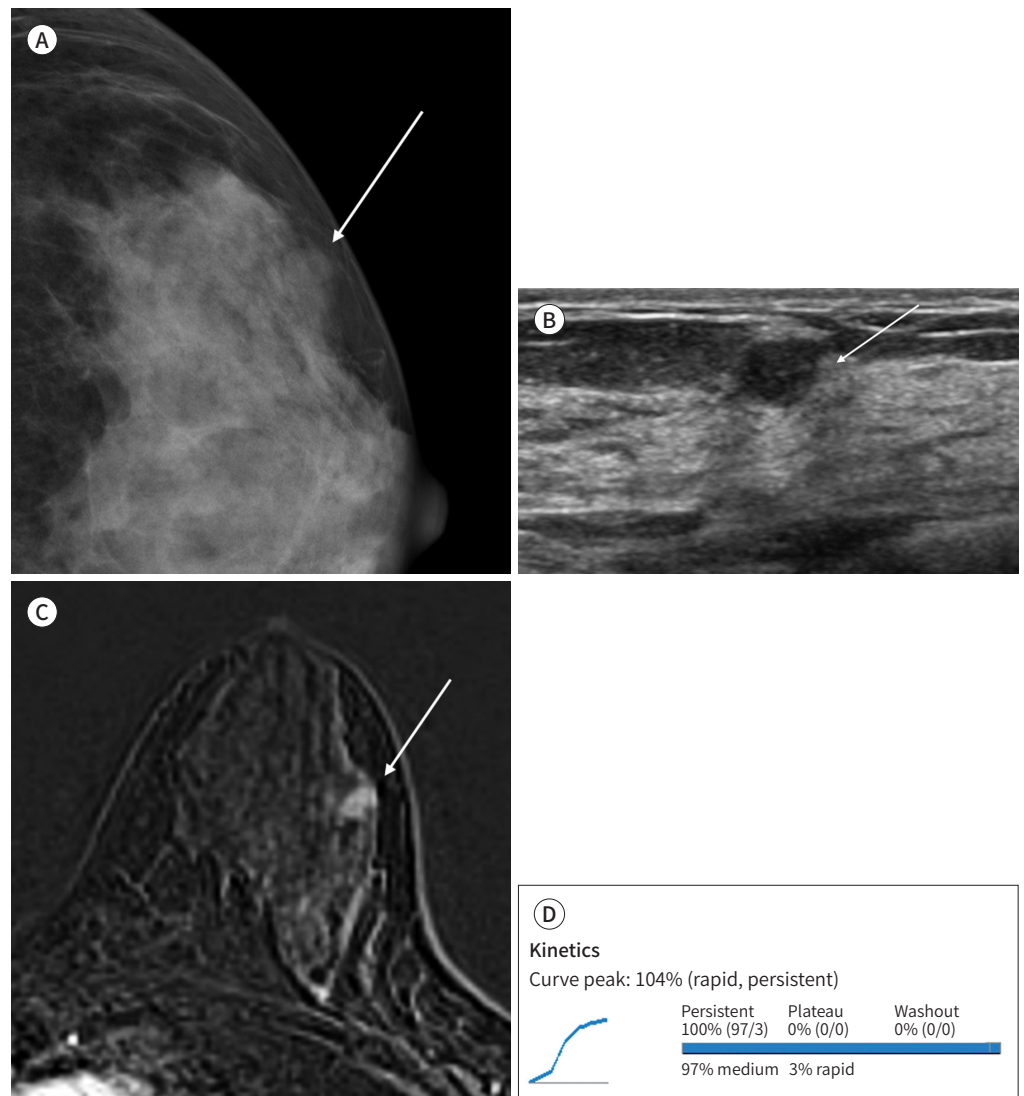
Fig. 1. A 41-year-old female diagnosed with lobular carcinoma in situ of the left breast.

A. Mammogram shows an oval circumscribed isodense mass without microcalcification (arrow) in the craniocaudal view.

B. Ultrasound image shows an oval circumscribed isoechoic mass (arrow) in the left breast.

C. Early-phase axial dynamic contrast-enhanced MRI subtraction image shows a mass with irregular margins and homogeneous enhancement (arrow).

D. MRI with a computer-aided diagnosis color overlay map shows 104% peak enhancement and a 100% persistent component.

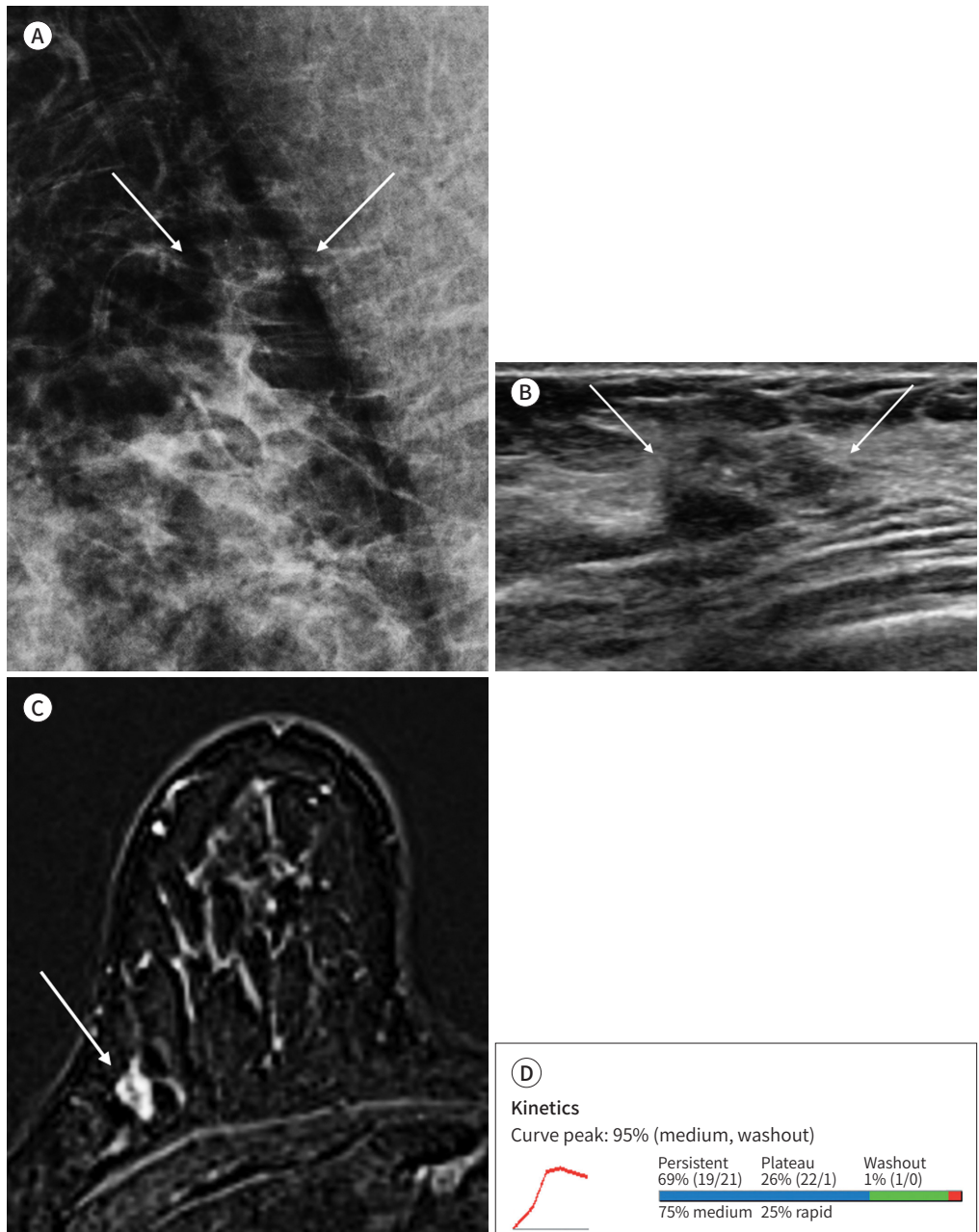


$p = 0.033$), and US features including oval or round shape (OR = 4.098, $p = 0.032$), parallel orientation (OR = 5.464, $p = 0.005$), and isoechoic texture (OR = 3.360, $p = 0.029$) remained significant independent factors associated with LCIS (Supplementary Table 2 in the online-only Data Supplement). The area under the ROC curve for distinguishing LCIS from ILC was 0.904 (95% confidence interval, 0.857–0.951) (Fig. 4).

Subgroup analysis in patients with lesions ≤ 1 cm showed that features on mammography more frequent in patients with smaller LCIS than with smaller ILC included unseen lesion or calcification alone; circumscribed mass; and amorphous calcification. US features more fre-

quent in smaller LCIS than smaller ILC included unseen, oval, or round shape lesions; circumscribed isoechoic masses with parallel orientation; and absence of posterior features. In addition, unseen lesions and homogeneous NME enhancement on MRI were associated with smaller LCIS.

Fig. 2. A 38-year-old female diagnosed with invasive lobular carcinoma in the right breast.
A. Mammogram shows an irregular isodense mass with microcalcifications (arrows) in the mediolateral view.
B. Ultrasound image shows an irregular and spiculated heterogeneous echoic mass (arrows) in the right breast.
C. Early-phase axial dynamic contrast-enhanced MRI subtraction image shows an irregular mass with spiculated margins and heterogeneous enhancement (arrow).
D. MRI with a computer-aided diagnosis color overlay map shows a 95% peak enhancement and a 4% washout component.



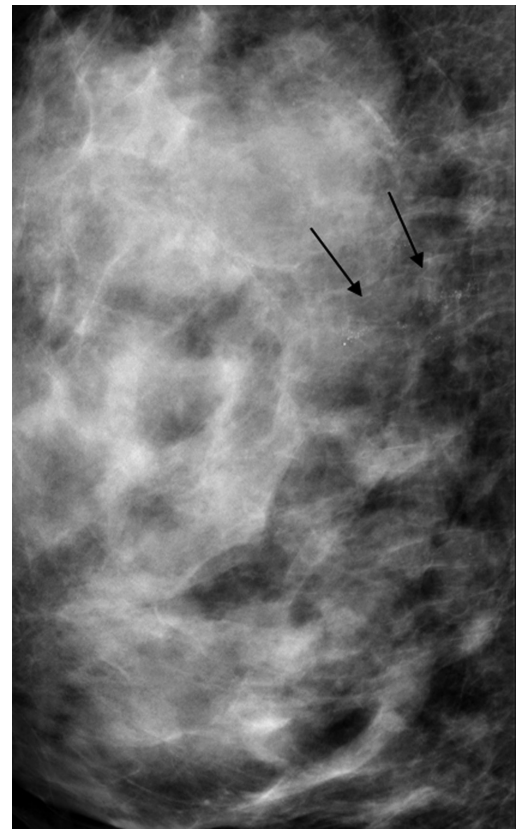


Fig. 3. A 45-year-old female diagnosed with lobular carcinoma in situ in the left breast. Mammogram shows grouped amorphous microcalcifications in the mediolateral view (arrows).

DISCUSSION

This study demonstrates imaging differences between LCISs and ILCs ≤ 2 cm. US features, including oval or round shape (OR = 4.098), parallel orientation (OR = 5.464), and isoechotexture (OR = 3.360), as well as smaller lesion size (OR = 1.103) and younger age (OR = 1.100), were independent variables associated with small LCIS. Subgroup analysis in patients with lesions ≤ 1 cm showed that benign features were significantly more common in the LCIS than in the ILC group.

Breast US showed that small LCISs and small ILCs exhibit distinct morphological features. The major US findings of LCIS have been reported to include irregular shape, hypoechoic echotexture, avascularity, and posterior shadowing (13, 14). LCIS lesions in this study also showed hypoechoic echotexture more frequently. Other features favoring benign lesions, including oval or round shape, parallel orientation, and isoechotexture, were not observed in the LCIS group. These discrepancies may be related to our selection of smaller-sized LCISs and the small number of patients included in other studies. In study from Scoggins et al. (13), there were 22 small lesions (less than 2 cm) of 31 LCISs in 26 female ranging in from 0.3 cm to 10 cm. Choi et al. (14) reported that the size of LCIS varied from 0.4 cm to 1.6 cm in 9 patients. An isoechoic pattern was more common in LCISs than in ILCs ≤ 1 cm in size, suggesting that this US feature may help differentiate small LCISs from small ILCs.

Studies have shown that the most common findings in LCISs included calcifications with

Table 3. Ultrasound Features of Female with LCISs and ILCs

	Total			Lesion Size ≤ 1 cm			Lesion Size > 1 cm		
	LCIS (n = 52)	ILC (n = 180)	p	LCIS (n = 39)	ILC (n = 42)	p	LCIS (n = 13)	ILC (n = 138)	p
Lesion type			< 0.001			0.001			0.054
Not seen	13/52 (25.0)	1/180 (0.1)		12/39 (30.8)	1/42 (2.38)		1/13 (7.7)	0/138 (0.0)	
Mass	36/52 (69.2)	171/180 (95.0)		25/39 (64.1)	37/42 (88.1)		11/13 (84.6)	134/138 (97.1)	
Non-mass	3/52 (5.8)	7/180 (3.9)		2/39 (5.1)	4/42 (9.5)		1/13 (7.7)	3/138 (2.2)	
Mixed	0/52 (0.0)	1/180 (0.1)		0/39 (0.0)	0/42 (0.0)		0/13 (0.0)	1/138 (0.7)	
Multifocal or multicentric			0.224			0.542			0.756
Absent	32/39 (82.1)	127/179 (71.0)		23/27 (85.2)	32/41 (78.1)		9/12 (75.0)	95/138 (68.8)	
Present	7/39 (18.0)	52/179 (29.1)		4/27 (14.8)	9/41 (22.0)		3/12 (25.0)	43/138 (31.2)	
Mass shape			< 0.001			0.038			< 0.001
Oval or round	24/36 (66.7)	24/172 (14.0)		16/25 (64.0)	13/37 (35.1)		8/11 (72.7)	11/135 (8.2)	
Irregular	12/36 (33.3)	148/172 (86.1)		9/25 (36.0)	24/37 (64.9)		3/11 (27.3)	124/135 (91.9)	
Mass orientation			0.002			< 0.001			0.105
Parallel	32/36 (88.9)	103/172 (59.9)		22/25 (88.0)	14/37 (37.8)		10/11 (90.9)	89/135 (65.9)	
Not parallel	4/36 (11.1)	69/172 (40.1)		3/25 (12.0)	2/37 (62.2)		1/11 (9.1)	46/135 (34.1)	
Mass margin			< 0.001			< 0.001			0.013
Circumscribed	10/36 (27.8)	2/172 (1.2)		9/25 (36.0)	1/37 (2.7)		1/11 (9.1)	1/135 (0.7)	
Indistinct	5/36 (13.9)	41/172 (23.8)		4/25 (16.0)	3/37 (8.1)		1/11 (9.1)	38/135 (28.2)	
Angular	2/36 (5.6)	19/172 (11.1)		2/25 (8.0)	0/37 (0.0)		0/11 (0.0)	19/135 (14.1)	
Microlobulated	14/36 (38.9)	29/172 (16.9)		8/25 (32.0)	4/37 (10.8)		6/11 (54.6)	25/135 (18.5)	
Spiculated	5/36 (13.9)	81/172 (47.1)		2/25 (8.0)	29/37 (78.4)		3/11 (27.3)	52/135 (38.5)	
Echo pattern			< 0.001			0.002			0.226
Hypo	21/36 (58.3)	118/172 (68.6)		13/25 (52.0)	26/37 (70.3)		8/11 (72.7)	92/135 (68.2)	
Iso	12/36 (33.3)	5/172 (2.9)		11/25 (44.0)	3/37 (8.1)		1/11 (9.1)	2/135 (1.5)	
Heterogeneous	3/36 (8.3)	49/172 (28.5)		1/25 (4.0)	8/37 (21.6)		2/11 (18.2)	41/135 (30.4)	
Posterior features			< 0.001			0.009			0.004
None	32/39 (82.1)	100/179 (55.9)		23/27 (85.2)	28/41 (68.3)		9/12 (75.0)	72/138 (52.2)	
Enhancement	6/39 (15.4)	10/179 (5.6)		3/27 (11.1)	1/41 (2.4)		3/12 (25.0)	9/138 (6.5)	
Shadowing	1/39 (2.6)	68/179 (38.0)		1/27 (3.7)	12/41 (29.3)		0/12 (0.0)	56/138 (40.6)	
Combined	0/39 (0.0)	1/179 (0.1)		0/27 (0.0)	0/41 (0.0)		0/12 (0.0)	1/138 (0.7)	
Vascularity			0.286			0.338			0.310
Absent	32/39 (82.1)	136/179 (76.0)		24/27 (88.9)	32/41 (78.1)		8/12 (66.7)	104/138 (75.4)	
Internal vascularity	6/39 (15.4)	24/179 (13.4)		3/27 (11.1)	9/41 (22.0)		3/12 (25.0)	15/138 (10.9)	
Vessels in rim	1/39 (2.6)	19/179 (10.6)		0/27 (0.0)	0/41 (0.0)		1/12 (8.3)	19/138 (13.8)	

Results are reported as the number (percentage) of patients.

ILC = invasive lobular carcinoma, LCIS = lobular carcinoma in situ

amorphous (15%–42%) or coarse heterogeneous (15%–26%) or pleomorphic (3%–69%) morphologies and grouped distribution (65%) (13-16). Although our multivariate analysis found that the presence of calcifications, calcification morphology, and distribution were not significantly associated with small LCISs, the percentages of lesions with calcification, amorphous or fine pleomorphic morphologies, and grouped distribution were higher in the small LCIS group than in the small ILC group, consistent with previous findings (13-16). Subgroup

Table 4. MRI Features of Female with LCISs and ILCs

	Total			Lesion Size ≤ 1 cm			Lesion Size > 1 cm		
	LCIS (n = 20)	ILC (n = 150)	p	LCIS (n = 10)	ILC (n = 34)	p	LCIS (n = 10)	ILC (n = 116)	p
Background parenchymal enhancement			0.295			> 0.999			0.134
Minimal or mild	15/20 (5.0)	130/150 (86.7)		8/10 (80.0)	28/34 (82.4)		7/10 (70.0)	102/116 (87.9)	
Moderate or marked	5/20 (25.0)	20/150 (13.3)		2/10 (20.0)	6/34 (17.7)		3/10 (30.0)	14/116 (12.1)	
Multifocal or multicentric			0.146			0.092			0.725
Absent	18/20 (90.0)	108/150 (72.0)		10/10 (100.0)	25/34 (73.5)		8/10 (80.0)	83/116 (71.6)	
Present	2/20 (10.0)	42/150 (28.0)		0/10 (0.0)	9/34 (26.5)		2/10 (20.0)	33/116 (28.5)	
Lesion type			< 0.001			0.009			0.021
Not seen	3/20 (15.0)	0/150 (0.0)		3/10 (30.0)	0/34 (0.0)		0/10 (0.0)	0/116 (0.0)	
Mass	12/20 (60.0)	136/150 (90.7)		5/10 (50.0)	29/34 (85.3)		7/10 (70.0)	107/116 (92.2)	
NME	5/20 (25.0)	7/150 (4.7)		2/10 (20.0)	4/34 (11.8)		3/10 (30.0)	3/116 (2.6)	
Mass with NME	0/20 (0.0)	7/150 (4.7)		0/10 (0.0)	1/34 (2.9)		0/10 (0.0)	6/116 (5.2)	
Mass shape			0.023			0.630			0.078
Oval, or round	7/12 (58.3)	34/143 (23.8)		4/5 (80.0)	18/30 (60.0)		3/7 (42.9)	16/113 (14.2)	
Irregular	5/12 (41.7)	109/143 (76.2)		1/5 (20.0)	12/30 (40.0)		4/7 (57.1)	97/113 (85.8)	
Mass margin			0.001			0.404			0.021
Circumscribed	5/12 (41.7)	12/143 (8.4)		3/5 (60.0)	8/30 (26.7)		2/7 (28.6)	4/113 (3.5)	
Irregular	3/12 (25.0)	89/143 (62.2)		1/5 (20.0)	14/30 (46.7)		2/7 (28.6)	75/113 (66.4)	
Spiculated	4/12 (33.3)	42/143 (29.4)		1/5 (20.0)	8/30 (26.7)		3/7 (42.9)	34/113 (30.1)	
Mass internal enhancement			0.122			0.562			0.047
Homogeneous	7/12 (58.3)	44/143 (30.8)		2/5 (40.0)	15/30 (50.0)		5/7 (71.4)	29/113 (25.7)	
Heterogeneous	3/12 (25.0)	75/143 (52.5)		1/5 (20.0)	10/30 (33.3)		2/7 (28.6)	65/113 (57.5)	
Rim	2/12 (16.7)	24/143 (16.8)		2/5 (40.0)	5/30 (16.7)		0/7 (0.0)	19/113 (16.8)	
NME distribution			0.235			> 0.999			0.045
Focal	1/5 (20.0)	0/14 (0.0)		0/2 (0.0)	0/5 (0.0)		1/3 (33.3)	0/9 (0.0)	
Linear	1/5 (20.0)	1/14 (7.1)		0/2 (0.0)	0/5 (0.0)		1/3 (33.3)	1/9 (11.1)	
Segmental	2/5 (40.0)	11/14 (78.6)		2/2 (100.0)	4/5 (80.0)		0/3 (0.0)	7/9 (77.8)	
Multiple region	1/5 (20.0)	2/14 (14.3)		0/2 (0.0)	1/5 (20.0)		1/3 (33.3)	1/9 (11.1)	
NME internal enhancement			0.031			0.048			0.236
Homogeneous	4/5 (80.0)	2/14 (14.3)		2/2 (100.0)	0/5 (0.0)		2/3 (66.7)	2/9 (22.2)	
Heterogeneous	1/5 (20.0)	12/14 (85.7)		0/2 (0.0)	5/5 (100.0)		1/3 (33.3)	7/9 (77.8)	
Kinetics			< 0.001			0.490			< 0.001
Persistent	10/17 (58.8)	15/150 (10.0)		3/7 (42.9)	7/34 (20.6)		7/10 (70.0)	8/116 (6.9)	
Plateau	1/17 (5.9)	26/150 (17.3)		1/7 (14.3)	10/34 (29.4)		0/10 (0.0)	16/116 (13.8)	
Washout	6/17 (35.3)	109/150 (72.7)		3/7 (42.9)	17/34 (50.0)		3/10 (30.0)	92/116 (79.3)	
Intratumoral high SI on T2WI			0.278			0.143			0.834
Absent	11/12 (91.7)	140/143 (97.9)		4/5 (80.0)	30/30 (100.0)		7/7 (100.0)	110/113 (97.3)	
Present	1/12 (8.3)	3/143 (3.7)		1/5 (20.0)	0/30 (0.0)		0/7 (0.0)	3/113 (2.8)	
Peritumoral edema on T2WI			0.517			0.857			0.649
Absent	12/12 (100.0)	135/143 (94.4)		5/5 (100.0)	29/30 (96.7)		10/10 (100.0)	106/113 (93.8)	
Present	0/12 (0.0)	8/143 (5.5)		0/5 (0.0)	1/30 (3.3)		0/10 (0.0)	7/113 (5.8)	

Results are reported as the number (percentage) of patients.

ILC = invasive lobular carcinoma, LCIS = lobular carcinoma in situ, NME = nonmass enhancement, SI = signal intensity, T2WI = T2-weighted imaging

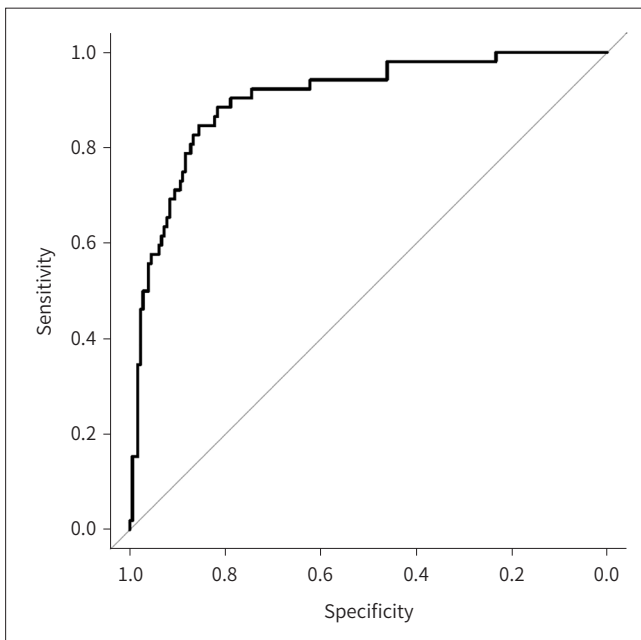


Fig. 4. ROC curve for distinguishing a small lobular carcinoma in situ from a small invasive lobular carcinoma. The area under the ROC curve is 0.904 (95% confidence interval, 0.857–0.951). ROC = receiver operating characteristic

analysis showed that calcification rates were higher in LCISs ≤ 1 cm than > 1 cm in size. Up to 41% of lobular neoplasias were reported to have calcifications within the neoplastic cells, with these calcifications possibly reflected on mammography (23). LCISs are often incidentally identified during removal of breast tissue samples for other proliferative lesions with calcifications, such as FEA and columnar cell lesions. Lobular neoplasias, including LCISs, are genetically and molecularly associated with FEA and columnar cell lesions, forming a low-grade breast neoplasia family (24). Thus, the presence of calcifications may also be associated with other concurrent proliferative lesions.

In this study, mass lesion was the most common MRI finding of small LCIS. Features favoring benign lesions, including oval or round shape, circumscribed margins, homogeneous enhancement, and persistent kinetics, were more frequent in the small LCIS than in the small ILC group. Although NME (five of seven, 71%) was the most frequent finding in LCISs from study of Scoggins et al. (13), the numbers of patients in that study and in ours were too small to draw any conclusions. Further validation is needed for diagnosis and differentiation of small LCIS.

This study had several limitations. First, this study was of retrospective design and was conducted at a single tertiary referral center. Second, the LCIS group included not only pure LCIS lesions, but also those with other types of low-grade breast neoplasia, including concurrent FEA and/or columnar cell lesions. However, LCIS is genetically and molecularly associated with FEA and columnar cell lesions (24). Third, the number of patients undergoing MRI was small. Thus, variables associated with MRI were not included in the univariate and multivariate analyses. Finally, we included the cases confirmed by stereotactic vacuum-assisted biopsy and these cases may show almost the tumor excised after the procedure before performing the breast US and MRI.

In conclusion, small LCIS tumors tend to demonstrate more benign features than small

ILCs. Several imaging features were independent variables that may predict LCIS and may help differentiate between small LCISs and ILCs.

Supplementary Materials

The online-only Data Supplement is available with this article at <http://dx.doi.org/10.3348/jksr.2020.0148>.

Author Contributions

Conceptualization, Y.G.Y., C.J.H., K.H.H., B.M.S.; formal analysis, Y.G.Y., C.J.H.; investigation, Y.G.Y., C.J.H.; methodology, Y.G.Y., C.J.H., K.H.H.; resources, Y.G.Y., C.J.H.; supervision, C.J.H.; validation, all authors; visualization, Y.G.Y., C.J.H., L.H.J., G.G.; writing—original draft, Y.G.Y.; and writing—review & editing, all authors.

Conflicts of Interest

Hak Hee Kim has been a Section Editor of the Journal of the Korean Society of Radiology since 2012; however, she was not involved in the peer reviewer selection, evaluation, or decision process of this article. Otherwise, no other potential conflicts of interest relevant to this article were reported.

Funding

None

REFERENCES

1. Foote FW, Stewart FW. Lobular carcinoma in situ: a rare form of mammary cancer. *Am J Pathol* 1941;17:491-496
2. Giuliano AE, Connolly JL, Edge SB, Mittendorf EA, Rugo HS, Solin LJ, et al. Breast cancer—major changes in the American Joint Committee on Cancer eighth edition cancer staging manual. *CA Cancer J Clin* 2017;67:290-303
3. Mann RM, Loo CE, Wobbes T, Bult P, Barentsz JO, Gilhuijs KG, et al. The impact of preoperative breast MRI on the re-excision rate in invasive lobular carcinoma of the breast. *Breast Cancer Res Treat* 2010;119:415-422
4. Hwang ES, Nyante SJ, Yi Chen Y, Moore D, DeVries S, Korkola JE, et al. Clonality of lobular carcinoma in situ and synchronous invasive lobular carcinoma. *Cancer* 2004;100:2562-2572
5. Sakr RA, Schizas M, Carniello JV, Ng CK, Piscuoglio S, Giri D, et al. Targeted capture massively parallel sequencing analysis of LCIS and invasive lobular cancer: repertoire of somatic genetic alterations and clonal relationships. *Mol Oncol* 2016;10:360-370
6. Lopez-Garcia MA, Geyer FC, Lacroix-Triki M, Marchió C, Reis-Filho JS. Breast cancer precursors revisited: molecular features and progression pathways. *Histopathology* 2010;57:171-192
7. National Comprehensive Cancer Network. NCCN clinical practice guidelines in oncology: breast cancer. version 1. Available at: https://www.nccn.org/professionals/physician_gls/pdf/breast.pdf. Published 2019. Accessed Jun 26, 2019
8. Nagi CS, O'Donnell JE, Tismenetsky M, Bleiweiss IJ, Jaffer SM. Lobular neoplasia on core needle biopsy does not require excision. *Cancer* 2008;112:2152-2158
9. Hwang H, Barke LD, Mendelson EB, Susnik B. Atypical lobular hyperplasia and classic lobular carcinoma in situ in core biopsy specimens: routine excision is not necessary. *Mod Pathol* 2008;21:1208-1216
10. Karabakhtsian RG, Johnson R, Sumkin J, Dabbs DJ. The clinical significance of lobular neoplasia on breast core biopsy. *Am J Surg Pathol* 2007;31:717-723
11. O'Neil M, Madan R, Tawfik OW, Thomas PA, Fan F. Lobular carcinoma in situ/atypical lobular hyperplasia on breast needle biopsies: does it warrant surgical excisional biopsy? A study of 27 cases. *Ann Diagn Pathol* 2010;14:251-255
12. Hussain M, Cunnick GH. Management of lobular carcinoma in-situ and atypical lobular hyperplasia of the breast—a review. *Eur J Surg Oncol* 2011;37:279-289
13. Scoggins M, Krishnamurthy S, Santiago L, Yang W. Lobular carcinoma in situ of the breast: clinical, radio-

- logical, and pathological correlation. *Acad Radiol* 2013;20:463-470
14. Choi BB, Kim SH, Park CS, Cha ES, Lee AW. Radiologic findings of lobular carcinoma in situ: mammography and ultrasonography. *J Clin Ultrasound* 2011;39:59-63
 15. Maxwell AJ, Clements K, Dodwell DJ, Evans AJ, Francis A, Hussain M, et al. The radiological features, diagnosis and management of screen-detected lobular neoplasia of the breast: findings from the Sloane Project. *Breast* 2016;27:109-115
 16. Amos B, Chetlen A, Williams N. Atypical lobular hyperplasia and lobular carcinoma in situ at core needle biopsy of the breast: an incidental finding or are there characteristic imaging findings? *Breast Dis* 2016; 36:5-14
 17. Abdel-Fatah TM, Powe DG, Hodi Z, Lee AH, Reis-Filho JS, Ellis IO. High frequency of coexistence of columnar cell lesions, lobular neoplasia, and low grade ductal carcinoma in situ with invasive tubular carcinoma and invasive lobular carcinoma. *Am J Surg Pathol* 2007;31:417-426
 18. Abdel-Fatah TM, Powe DG, Hodi Z, Reis-Filho JS, Lee AH, Ellis IO. Morphologic and molecular evolutionary pathways of low nuclear grade invasive breast cancers and their putative precursor lesions: further evidence to support the concept of low nuclear grade breast neoplasia family. *Am J Surg Pathol* 2008;32:513-523
 19. D'Orsi CJ, Sickles EA, Mendelson EB, Morris EA, American College of Radiology. *ACR BI-RADS® atlas: breast imaging reporting and data system*. 5th ed. Reston, VA: American College of Radiology 2013
 20. Choe J, Chikarmane SA, Giess CS. Nonmass findings at breast US: definition, classifications, and differential diagnosis. *Radiographics* 2020;40:326-335
 21. Uematsu T, Kasami M, Yuen S. Triple-negative breast cancer: correlation between MR imaging and pathologic findings. *Radiology* 2009;250:638-647
 22. Baltzer PA, Yang F, Dietzel M, Herzog A, Simon A, Vag T, et al. Sensitivity and specificity of unilateral edema on T2w-TSE sequences in MR-mammography considering 974 histologically verified lesions. *Breast J* 2010;16:233-239
 23. Crisi GM, Mandavilli S, Cronin E, Ricci A Jr. Invasive mammary carcinoma after immediate and short-term follow-up for lobular neoplasia on core biopsy. *Am J Surg Pathol* 2003;27:325-333
 24. Dabbs DJ, Oesterreich S. *Lobular neoplasia and invasive lobular carcinoma*. In: Dabbs DJ, ed. *Breast pathology*. 2nd ed. Philadelphia, PA: Elsevier 2017:436-470

유방의 소엽상피내암과 침윤성 소엽암의 영상의학적 소견 비교

윤가영¹ · 차주희^{2*} · 김학희² · 방민서³ · 이희진⁴ · 공경엽⁴

목적 크기가 작은 소엽상피내암(lobular carcinoma in situ; 이하 LCIS)과 침윤성 소엽암(invasive lobular carcinoma; 이하 ILC)의 영상의학적 소견을 비교하여 감별에 도움을 줄 수 있는지 알아보았다.

대상과 방법 2012년 1월부터 2016년 12월까지 2 cm 이하의 LCIS 여성 환자 52명(중앙값 45세, 범위 32-67세)과 ILC 여성 환자 180명(중앙값 49세, 범위 36-75세)을 대상으로 하였다. 모든 환자는 유방촬영술과 초음파 검사를 받았고, LCIS 환자 20명과 ILC 환자 150명은 MRI 검사를 받았다. 두 집단의 임상적, 영상의학적 소견들을 비교했고, 병변 크기에 따라 소그룹으로 나눠 추가 분석하였다.

결과 LCIS 환자는 다변량 분석에서 나이가 적을수록(odds ratio [이하 OR] = 1.100), 종괴 크기가 작을수록(OR = 1.103), 종괴가 둥글거나 타원형일 때(OR = 4.098), 종괴가 피부선과 평행할 때(OR = 5.464), 지방과 동등한 에코일 때(OR = 3.360), 오즈비(OR)가 유의하게 높았다. 그룹 간 감별에서 receiver operating characteristic curve 아래 면적값은 0.904 (95% 신뢰 구간, 0.857-0.951)였다. 소그룹 분석에서 크기가 더 작은 LCIS (≤ 1 cm)는 ILC보다 양성에 가깝게 보였다.

결론 크기가 작은 LCIS는 ILC보다 양성에 가까운 소견들을 보였다. 몇 가지 영상의학적 소견은 LCIS를 예측과 관련된 독립인자로 생각된다.

¹울산대학교 의과대학 강릉아산병원 영상학과, ²울산대학교 의과대학 서울아산병원 ²영상학과, ⁴병리과, ³울산대학교 의과대학 울산대학교병원 영상학과